HHS Public Access

Author manuscript

Cell Rep. Author manuscript; available in PMC 2018 January 22.

Published in final edited form as:

Cell Rep. 2017 October 31; 21(5): 1281–1292. doi:10.1016/j.celrep.2017.10.028.

CNS Neurons Deposit Laminin α5 to Stabilize Synapses

Mitchell H. Omar[1,2], **Meghan Kerrisk Campbell**[2], **Xiao Xiao**[2], **Qiaonan Zhong**[3], **William J. Brunken**[6], **Jeffrey H. Miner**[7], **Charles A. Greer**[1,4,5], and **Anthony J. Koleske**[1,2,4,8,*]

[1]Interdepartmental Neuroscience Program, Yale University, New Haven, CT 06510, USA

[2]Department of Molecular Biophysics and Biochemistry, Yale University, New Haven, CT 06510, USA

[3]Department of Molecular, Cellular, and Developmental Biology, Yale University, New Haven, CT 06510, USA

[4]Department of Neuroscience, Yale University, New Haven, CT 06510, USA

[5]Department of Neurosurgery, Yale University, New Haven, CT 06510, USA

[6]Department of Ophthalmology, Upstate Medical University, Syracuse, NY 13202, USA

[7]Division of Nephrology, Department of Medicine, Washington University School of Medicine, St. Louis, MO 63110, USA

SUMMARY

Synapses in the developing brain are structurally dynamic but become stable by early adulthood. We demonstrate here that an α5-subunit-containing laminin stabilizes synapses during this developmental transition. Hippocampal neurons deposit laminin α5 at synapses during adolescence as connections stabilize. Disruption of laminin α5 in neurons causes dramatic fluctuations in dendritic spine head size that can be rescued by exogenous α5-containing laminin. Conditional deletion of laminin α5 *in vivo* increases dendritic spine size and leads to an age-dependent loss of synapses accompanied by behavioral defects. Remaining synapses have larger postsynaptic densities and enhanced neurotransmission. Finally, we provide evidence that laminin α5 acts through an integrin α3β1-Abl2 kinase-p190RhoGAP signaling cascade and partners with laminin β2 to regulate dendritic spine density and behavior. Together, our results identify laminin α5 as a stabilizer of dendritic spines and synapses in the brain and elucidate key cellular and molecular mechanisms by which it acts.

*Correspondence: anthony.koleske@yale.edu.
[8]Lead Contact

SUPPLEMENTAL INFORMATION

Supplemental Information includes Supplemental Experimental Procedures, four figures, and four movies and can be found with this article online at https://doi.org/10.1016/j.celrep.2017.10.028.

AUTHOR CONTRIBUTIONS

M.H.O., A.J.K., and M.K.C. designed the study. M.H.O. and A.J.K. wrote the paper. M.H.O., X.X., and M.K.C. conducted experiments and analyzed results. Q.Z. assisted with in situ hybridization and electron microscopy. C.A.G. provided logistical support for dendrite reconstructions and electron microscopy. W.J.B. and J.H.M. provided essential reagents and key advice. All authors approved the final manuscript.

In Brief

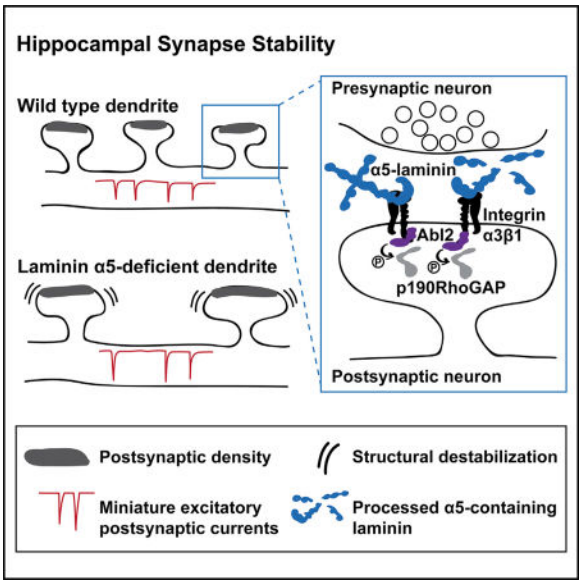

In the developing brain, synaptic structure transitions from dynamic to stable by early adulthood. Omar et al. identify a laminin molecule deposited at synapses in the brain that is essential for dendritic spine structural regulation and synapse stability between early postnatal development and adulthood.

INTRODUCTION

Developing synapses in the CNS are structurally dynamic but become more stable as the brain matures (Chen et al., 2014; Dailey and Smith, 1996; Grutzendler et al., 2002; Holtmaat et al., 2005; Majewska and Sur, 2003; Zuo et al., 2005). The extracellular molecules that confer stability on synapse and dendritic spine structure in the brain are largely unknown. Binding of integrin adhesion receptors to extracellular matrix (ECM) stabilizes cellular structures in a wide variety of biological contexts (Campbell and Humphries, 2011; Hynes, 2002), and our previous work found that integrin α3β1 is necessary for synapse stability in the late postnatal mouse brain (Kerrisk et al., 2013; Warren et al., 2012).

Integrin α3β1 is a receptor for laminins—secreted heterotrimeric ECM glycoproteins made up of α, β, and γ subunits—with highest affinity for those containing the α5 subunit (Nishiuchi et al., 2006). This suggests a possible role for laminin α5 in synapse stabilization. Laminins are major constituents of the basal lamina in many tissues, where they provide a substrate for cellular attachment and structural support (Sanes, 2003; Yurchenco, 2011). However, the limited size of the cleft at central synapses is too small to be congruent with a basal lamina and may be too restrictive for laminin in its fully extended conformation (Beck et al., 1990; Engel et al., 1981). For these reasons, major roles, if any, for laminins at central synapses have been controversial.

Here, we identify laminin α5 as a regulator of synapse stability in the brain during late postnatal development. We provide evidence that hippocampal neurons deposit laminin α5

at synapses, stabilizing dendritic spine structure after postnatal day 15 (P15) and synapse density between P21 and P42. Loss of laminin α5 and the ensuing loss of synapse stabilization also disrupts synaptic transmission and animal behavior, demonstrating it is essential for proper brain function. Finally, we provide evidence that laminin α5 signals through an integrin α3β1 adhesion receptor-Abl2 kinase-p190RhoGAP signaling pathway, and we find that laminin α5 and integrin α3 interact functionally to regulate dendritic spine density and animal behavior.

RESULTS

Hippocampal Neurons Deposit the ECM Protein Laminin α5 at Synapses

In situ hybridization with an antisense probe revealed extensive *Lama5* mRNA throughout the brain of P35 wild-type (WT) animals, primarily in neurons. In the hippocampus, signal was most prominent in the dentate gyrus and pyramidal layer, populated predominantly with excitatory neurons. Scattered cells, most likely interneurons, in strata oriens, radiatum, and lacunosum moleculare, were also positive for *Lama5* mRNA (Figure 1A), as were cells in the cortex and cerebellum (Figure S1A). Immunostaining dissociated hippocampal neurons at 21 days *in vitro* (DIV) prior to fixation or permeabilization revealed extracellular laminin α5 protein along dendritic processes at dendritic spines (Figure 1B). Co-staining for the presynaptic marker synaptophysin indicated that laminin α5 localizes to synaptic sites (Figure 1C). As a staining control, we used a *NEX-Cre* driver to inactivate a conditional "floxed" laminin α5 in excitatory forebrain neurons (e.g., *NEX-Cre*; $Lama5^{flox/flox}$, or *NEX-Lama5*$^{-/-}$) (Goebbels et al., 2006; Nguyen et al., 2005). Recombination of the laminin α5 allele was detected in hippocampus from *NEX-Lama5*$^{-/-}$ mice, but not in tail DNA (Figure S1B). Punctate laminin α5 staining in the hippocampus was decreased by 79% in sections from *NEX-Lama5*$^{-/-}$ mice compared to WT (Figures 1D and 1F). Furthermore, a ~70-kDa band that reacted with anti-laminin α5 antibodies was reduced by 70% in purified synaptic preparations from *NEX-Lama5*$^{-/-}$ mice relative to WT controls (Figures 1E, 1F, and S1C), reflecting loss of laminin α5 protein from excitatory neurons. This 70-kDa species showed highest levels at P17 and consistent lower levels from P25 through P85 (Figure S1D). Together, these data provide evidence that laminin α5 is produced by hippocampal neurons and that it localizes to synapses in the mouse brain.

Laminin α5 Is Delivered by the Postsynaptic Neuron

Co-staining for laminin α5 (extracellular) and Cre recombinase in hippocampal neurons cultured from *NEX-Lama5*$^{-/-}$ mice demonstrated a lack of laminin α5 staining on Cre-positive cells but a strong signal on Cre-negative cells, strongly suggesting that an α5-containing laminin can be deposited at synapses by the postsynaptic cell (Figure 1G). To test this hypothesis, we inserted a tag (Venus or 3xHA, which showed the same results) into the laminin α5 G2 domain and expressed the construct in hippocampal neurons. Tagged laminin α5 was distributed along dendrites of transfected neurons in a punctate pattern (Figure 1H) but was not detected in axons (Figure S2A). At DIV 10 (Figure 1H, top) and DIV 14 (not shown), Venus-laminin α5 localized to the base of spines in clusters along dendrites but became concentrated at the tips of dendritic spines only at later developmental time points (DIV 19; Figure 1H, bottom). We also measured laminin α5 staining in the reticular nucleus

of the thalamus, which is targeted by cortical neurons. No difference in staining intensity was found between P30 WT and *NEX-Lama5*$^{-/-}$ mice (Figures S2B and S2C). Given that *NEX-Cre* is expressed in the cortex, but not the thalamus, this observation provides further evidence that laminin α5 is provided by the postsynaptic partner. Together, these experiments strongly suggest laminin α5 is deposited at synapses via the dendrite of the postsynaptic neuron.

An α5-Containing Laminin Is Necessary and Sufficient for Decreasing Dendritic Spine Structural Fluctuations

Laminins stabilize cellular structure in a variety of biological contexts (Colognato and Yurchenco, 2000; Yao, 2017). Given the localization of laminin α5 at dendritic spines, we investigated a potential role for laminin α5 in the structural stability of dendritic spines by imaging GFP-filled dissociated hippocampal neurons from WT and *NEX-Lama5*$^{-/-}$ mice at DIV 21 at 4-min intervals. A reviewer blinded to genotype and condition measured fluorescence intensity of GFP in dendritic spine heads to estimate overall spine volume at each time point (Figures 2A and 2B; Movies S1 and S2). To determine the timescale of structural remodeling and the overall fold change in spine head size, we analyzed (1) the percent change from each time point to the following time point and (2) the ratio of maximum to minimum size for a spine over the course of 1 hr of imaging (Figure 2C). Dendritic spines on laminin α5-deficient neurons were significantly more dynamic than those on WT neurons, with larger percentage size changes between 4-min time points (Figure 2D) and larger overall ranges of size (Figure S3A). Importantly, the enhanced dynamic behavior of laminin α5-deficient neurons was suppressed by application of 3 nM recombinant α5-subunit-containing laminin heterotrimer (laminin α5β2γ1, or 521), but not by an α1-containing laminin (laminin α1β1γ1, or 111) (Figures 2E–2G and S2B; Movies S3 and S4). Together, these data suggest laminin α5 is both necessary and sufficient for stabilizing dendritic spine head size fluctuation in hippocampal neurons.

Integrin α3β1 can also bind laminin 332 (Nishiuchi et al., 2006). Application of 3 nM purified laminin 332 was sufficient to suppress both 4-min fluctuation and overall range of dendritic spine size change in neurons from *NEX-Lama5*$^{-/-}$ mice (Figures S3C and S3D). While there is evidence for *Lamb3* expression in hippocampus, *Lama3* and *Lamc2* are likely not expressed in hippocampus (Allen Mouse Brain Atlas). Thus, although laminin 332 can regulate dendritic spine structural stability, it likely does not do so endogenously in the hippocampus.

Loss of Laminin α5 Dysregulates Spine Head Size *In Vivo*

To understand the consequence of these structural changes, we tested how loss of laminin α5 impacted dendritic spine head size *in vivo* using electron microscopy (EM). Spine head cross-sectional area (Figure 2H) showed no difference between genotypes at P15 but was larger in *NEX-Lama5*$^{-/-}$ mice than in littermate WT controls at both P21 and P42 (Figure 2I, insets), with broader distributions of individual spine head measurements in *NEX-Lama5*$^{-/-}$ animals that were visible as reduced peaks and longer rightward tails (Figure 2I). These defects increased between P21 and P42 from a 21% to a 32% difference in head size.

Together, these data suggest that laminin α5 controls dendritic spine structural dynamics and that loss of laminin α5 dysregulates dendritic spine head size in the hippocampus.

Loss of Laminin α5 Disrupts Synapse Density and Function

Given the ability of laminin α5 to regulate dendritic spine structural dynamics and head size (Figure 2), we examined how its loss impacted synapses *in vivo*. We used electron microscopy to quantify the density (number per square micrometer) of excitatory synapses in hippocampal CA1 stratum radiatum of *NEX-Lama5*$^{-/-}$ mice and WT littermates (Figure 3A). While synapse densities were similar between these groups at P15 and P21, they were reduced by 24% in *NEX-Lama5*$^{-/-}$ mice relative to WT by P42 (Figure 3B). Consistent with this, miniature excitatory postsynaptic currents (mEPSCs) (Figure 3D) at Schaffer collateral-CA1 synapses were decreased in frequency by 25% in *NEX-Lama5*$^{-/-}$ neurons (Figure 3E) relative to WT. Interestingly, synapse density increased by 40% between P15 and P21 in WT animals, but no difference was detected between these time points in *NEX-Lama5*$^{-/-}$ animals (Figure 3B).

Postsynaptic density (PSD) length was greater in *NEX-Lama5*$^{-/-}$ mice relative to WT at all ages (Figure 3C), preceding the detectable defects in dendritic spine head size (Figure 2I) and synapse density (Figure 3B) in these mutants. Consistent with previous reports showing a correlation between PSD length and synaptic strength (Murthy et al., 2001), we found that α-amino-3-hydroxy-5-methyl-4-isoxazolepropionic acid receptor (AMPAR)-mediated mEPSC amplitudes were increased in *NEX-Lama5*$^{-/-}$ mice versus WT (Figure 3F, left). While NMDA receptor (NMDAR)-mEPSC amplitudes trended toward an increase in *NEX-Lama5*$^{-/-}$ mice, this difference was not significant ($p = 0.087$; Figure 3F, right). Decay times of AMPAR- and NMDAR-mediated mEPSCs were not different between genotypes (Figure S4A). Together, these results suggest that neuronal laminin α5 regulates synaptic size and transmission and that its loss disrupts synapse density in the hippocampus by early adulthood.

Given the reduction in synapses in *NEX-Lama5*$^{-/-}$ mice at P42, we tested how these changes impacted behavior in a hippocampus-dependent novel object recognition task (Broadbent et al., 2009; Cohen et al., 2013) (Figure 3G). *NEX-Lama5*$^{-/-}$ mice failed to discriminate between novel and familiar objects (Figure 3H), even though they performed similar to WT littermates on day 1 during object familiarization (Figure S4B) and spent similar amounts of time not exploring objects on the test day (Figure S4C). Because performance of this task requires intact hippocampal function (Cohen et al., 2013), failure of *NEX-Lama5*$^{-/-}$ mice in novel object recognition strongly suggests that forebrain excitatory neuron expression of laminin α5 is necessary for proper brain function.

Loss of Laminin α5 Disrupts Integrin α3β1-Abl2 Kinase-p190RhoGAP Signaling at Hippocampal Synapses

To directly address whether laminin α5 acts through the integrin α3β1 adhesion receptor to control synapse stability, we first compared levels of proteins in synaptosomal fractions from *NEX-Lama5*$^{-/-}$ and WT mice. We performed these experiments at P21 to avoid possible confounds resulting from the synapse loss at later ages. Integrin α3 levels were decreased by

25% in synaptosomes from *NEX-Lama5*$^{-/-}$ mice (Figures 4A and 4D). Levels of the integrin α3β1-interacting protein Abl2/Arg kinase (Abl2) (Kerrisk et al., 2013; Simpson et al., 2015; Warren et al., 2012) and phosphorylation of the Abl2 substrate p190RhoGAP (Hernández et al., 2004; Sfakianos et al., 2007) were also decreased by 24% and 22%, respectively (Figures 4B–4D). These decreases were selective, as levels of HSP70 and PSD95 were not significantly different between genotypes at this age (Figures 4E, 4F, and 4H). Levels of actin, however, were increased by 27% in *NEX-Lama5*$^{-/-}$ mice (Figures 4G and 4H), consistent with increased spine head and PSD sizes in *NEX-Lama5*$^{-/-}$ mice at this age.

Laminin α5 Interacts Functionally with Integrin α3 to Regulate Dendritic Spine Density and Animal Behavior

Laminin α5 and integrin α3 exhibit parallel peaks in levels at P17 in synaptosome fractions from WT hippocampus (Figure 5A) and parallel decreases at later time points, consistent with a functional interaction between these proteins. We investigated this relationship by reducing the gene dosage of *Lama5* and *Itga3* in combination and then testing for phenotypes in dendritic spine density and novel object recognition. *Lama5*$^{+/-}$*Itga3*$^{+/-}$ double-heterozygous mice had reduced dendritic spine density in CA1 stratum radiatum compared to WT mice or *Lama5*$^{+/-}$ or *Itga3*$^{+/-}$ single heterozygotes, which were both indistinguishable from WT (Figure 5B). Additionally, *Lama5*$^{+/-}$*Itga3*$^{+/-}$ mice failed novel object recognition while WT littermates and single-heterozygous littermates preferred the novel object (Figure 5C). The dose-sensitive interactions of *Lama5* with *Itga3* were selective, as *Lamc3*$^{+/-}$*Itga3*$^{+/-}$ double heterozygotes (*Lamc3* encodes the laminin γ3 subunit) did not exhibit deficits in novel object recognition. Finally, we note that laminin α5 can partner with the laminin β2 subunit in the laminin 521 trimer (Aumailley, 2013), which stabilized dendritic spines (Figure 2). We found *Lamb2*$^{+/-}$*Itga3*$^{+/-}$ double heterozygotes exhibited reduced dendritic spine density and defects in novel object recognition (Figures 5B and 5C), suggesting laminin β2 partners with laminin α5 to promote integrin-mediated dendritic spine and synapse stability.

DISCUSSION

Synapses in the developing brain are structurally dynamic, as they form, enlarge, shrink, and disappear during network formation and refinement. But as postnatal development progresses, synapses transition to a less dynamic, more stable state (Chen et al., 2014; Dailey and Smith, 1996; Grutzendler et al., 2002; Holtmaat et al., 2005; Majewska and Sur, 2003; Zuo et al., 2005). The molecules and mechanisms that enable structural stabilization in this transition are not well understood. Here, we provide evidence that an α5-containing laminin is critical to stabilization of dendritic spine structure and long-term synapse stability. We show that laminin α5 is expressed by neurons, localizes to synapses, and is deposited to its extracellular sites by the postsynaptic neuron during late postnatal development. Its peak in expression coincides with a 40% increase in synapse density that does not occur *NEX-Lama5*$^{-/-}$ mice (Figure 3B), suggesting laminin α5 may be needed to establish a stable synapse or convert a nascent synapse to a lasting one. Loss of laminin α5 function disrupts normal dendritic spine stability, leading to increased fluctuations in dendritic spine size that

are selectively attenuated by exogenous application of laminin 521. Further, mice lacking laminin α5 have normal synapse density at P21 but significantly fewer synapses than WT mice by P42. The synapses in these mice are larger, have increased AMPA currents, and have larger spine heads by P21. In addition, by P42, these mice fail a hippocampus-dependent behavioral task. We provide evidence that laminin α5 signals through an integrin α3β1 receptor-Abl2 signaling module to promote synapse stability *in vivo* and that laminin β2 may partner with laminin α5 during stabilization. Together, our data support a model (Figure 6) in which laminin α5 is a key coordinator of increasing synaptic stability during late postnatal development and that disruption of this transition compromises long-term synaptic stability *in vivo*.

Laminin α5 Plays Distinct Roles at Central Versus Peripheral Synapses

Previous work established roles for laminins in the development and organization of the large peripheral neuromuscular junction (NMJ) synapse (Martin et al., 1995; Nishimune et al., 2004, 2008; Noakes et al., 1995; Patton et al., 1997, 1998, 2001; Rogers and Nishimune, 2017; Tsai et al., 2012; Vezina-Audette et al., 2017). Several different laminin isoforms play discrete roles in NMJ development, organizing the pre- and postsynaptic compartments and providing key structural support. At the NMJ, loss of laminin α5 causes defects at P21, but after P40, these defects are not detected, and no further defects are observed (Nishimune et al., 2008). In contrast, we found deletion of laminin α5 from excitatory neurons in the forebrain leads to increased PSD size defects as early as P15, but synapse numbers are reduced, and defects in synaptic structure are greatly exacerbated, by P42. These dissimilar phenotypes may be due to differences such as different receptors, fundamentally different postsynaptic structures, and different molecular makeup of the synaptic cleft.

Laminins at the NMJ are organized into a basal lamina, which contains glycoproteins and proteoglycans and fills much of the 50 nm NMJ cleft (Sanes, 2003). In contrast, central synapses are much smaller than the NMJ and have no detectable basal lamina. Synaptic clefts in the CNS are only ~20 nm thick and thus may be unable to accommodate fully extended intact laminin trimers, which are >100 nm in length and >70 nm in width (Beck et al., 1990; Engel et al., 1981; Yurchenco and Schittny, 1990). Interestingly, we find that *NEX-Lama5*$^{-/-}$ mice have reduced levels of a 70-kDa laminin species (containing the more N-terminal L4a domain) in biochemically enriched synaptic fractions of hippocampus and that a construct containing the C-terminal G2 domain localizes to dendritic spines in transfected neurons (Figure 1H). These results suggest laminin α5 may function in a proteolyzed form at central synapses, which could be more reasonably accommodated at a 20 nm cleft, thereby avoiding the size constraints of a full-size trimer.

Similar to NMJ laminins, we find that laminin α5 is supplied by the postsynaptic partner (Nishimune et al., 2008). This is the most logical route for a large protein synthesized in the soma, since delivery to a dendritic spine would in most cases be less distance than delivery to an axonal terminal. This sorting appears to be very strict, as our data demonstrate even overexpressed laminin α5 rarely makes it into the axon hillock, and we observed no instances of axonal localization more distal to the soma. These observations could suggest a minus-end-directed, dynein-driven transport mechanism, such as that utilized by AMPA

receptors (Kapitein et al., 2010). This is an attractive hypothesis, as minus-end-out microtubules are less frequent in distal dendrites (Kapitein and Hoogenraad, 2011), and both endogenous and overexpressed laminin α5 is more prominent in proximal to mid-distance dendrites in our assays (Figures 1G and Figure S2A).

Laminin α5 Regulates Synapse Stability through an Integrin-Abl2 Pathway

Integrin adhesion receptors have important roles in the brain (Chan et al., 2006, 2007; Cingolani et al., 2008; Huang et al., 2006; Michaluk et al., 2009; Mortillo et al., 2012; Park and Goda, 2016; Pozo et al., 2012; Shi and Ethell, 2006). However, we lack clear evidence of the ligands for many of these receptors. In particular, integrin α3β1 binds Abl2/Arg kinase, which phosphorylates p190RhoGAP, a signaling axis critical for synapse stability (Kerrisk et al., 2013; Sfakianos et al., 2007; Warren et al., 2012). Our biochemical data suggest that disruption of laminin α5 reduces integrin α3β1 and Abl2 levels at synapses, possibly because loss of this ligand results in fewer anchor points for integrin α3β1 (Figure 6). We also find a decrease in tyrosine phosphorylation of p190RhoGAP. This is consistent with our previous finding that p190RhoGAP interacts functionally with Abl2 to control synapse and dendritic spine development (Sfakianos et al., 2007). Mice with reduced Abl2 and p190RhoGAP function have decreased synapse density and a broader distribution of spine head sizes in hippocampal CA1 stratum radiatum, phenotypes that closely resemble our findings here in *NEX-Lama5*$^{-/-}$ mice. Combined with our biochemical and genetic evidence (Figures 4 and 5), this suggests laminin α5 is deposited by the neuron to activate an integrin α3β1-Abl2-p190RhoGAP pathway that acts locally to stabilize the spine.

Interestingly, we show that another integrin α3β1-binding laminin, laminin 332 (Nishiuchi et al., 2006), can suppress enhanced dendritic spine size fluctuations. When taken together with the insufficiency of laminin 111 (which does not bind integrin α3β1), this provides another piece of evidence that laminin α5 is likely signaling through integrin α3β1 to control spine structural regulation in the hippocampus. These data also raise the possibility of other laminins acting in synaptic stabilization in the brain. While laminin α3 might not be expressed in the hippocampus, its mRNA is detected in the adult olfactory bulb (Allen Mouse Brain Atlas), hinting at a possible role there.

We also present genetic evidence that integrin α3β1 functionally interacts with laminins α5 and β2 to regulate dendritic spine density and mouse behavior. Given their size and number of protein-protein interaction domains, α5-containing laminins could signal through additional receptors to perform other roles at central synapses, accomplishing both autocrine (postsynaptic) and paracrine (presynaptic or glial) actions. The β2 subunit, for example, interacts with a presynaptic voltage-gated calcium channel at synapses (Nishimune et al., 2004). Other possible receptors for laminin α5 trimers and their proteolytic products in the brain include distinct laminin-binding integrin receptors, the dystroglycan receptor complex present at inhibitory synapses (Lévi et al., 2002), and lutheran/basal cell adhesion molecule (Moulson et al., 2001), all of which interact with laminin α5 in other biological contexts.

What Factors Regulate Laminin α5 Synthesis and Function at Central Synapses?

Fluctuations in dendritic spine head size are significantly increased in laminin α5-deficient neurons, but the addition of recombinant α5-containing laminin trimer selectively stabilizes dendritic spine head motility within minutes. These data strongly suggest that an α5-laminin acts directly at the synapse to promote stability. We also find that laminin α5 is deposited at hippocampal synapses between DIV14 and DIV19, and laminin α5 levels peak between P13 and P21, coinciding with both the maturation of dendritic spines and synapses and with the large increase in synapse density observed between P15 and P21 (Figure 3B). These findings raise the question of what factors or processes promote synaptic localization of laminin α5. Due to the effect of synaptic activity on stabilizing nascent structures (Roberts et al., 2010; Tropea et al., 2010; Yoshihara et al., 2009), it is possible that increased activity at newly functional synapses could induce neurons to deposit laminin α5 and dampen spine head dynamics. However, even mature synapses undergo structural changes in response to altered activity (Bosch and Hayashi, 2012; Colgan and Yasuda, 2014; Hayashi-Takagi et al., 2015; Lai and Ip, 2013; Matsuzaki et al., 2004; Nägerl et al., 2004; Zhou et al., 2004). Our findings suggest that laminin-integrin anchors at synapses would need to be disrupted to allow changes in spine size. In this regard, matrix metalloproteinases and plasmin/tissue plasminogen activator (tPA) have been shown to digest laminins, and both are regulated by activity and impact dendritic spine plasticity (Chen et al., 2008; Dziembowska and Wlodarczyk, 2012; Huntley, 2012; Levy et al., 2014; Magnowska et al., 2016; Oray et al., 2004; Wlodarczyk et al., 2011). We speculate that after early neurodevelopment, proteolysis of laminin α5 may disrupt laminin-integrin contacts to facilitate structural plasticity at stable central synapses.

Conclusions

Synaptic structure becomes less dynamic as postnatal development progresses. Here, we identify laminin α5 as a regulator of synapse stability in the brain after late postnatal development. We demonstrate that an α5-containing molecule signals via an integrin-α3β1-mediated pathway to stabilize synapses and impact function in the developing mouse hippocampus (Figure 6). Identification of this key mechanism for stabilizing synapse structure provides an entry point to further explore how synaptic structure is controlled and how it becomes dysregulated in disorders where synapse stability is compromised.

EXPERIMENTAL PROCEDURES

See Supplemental Experimental Procedures for full descriptions of our methods and resources.

Mice

Conditional allele *Lama5* mice (Nguyen et al., 2005) and NEX-Cre mice (Goebbels et al., 2006) were crossed to produce NEX-Cre;*Lama5*$^{flox/flox}$ mice, referred to as *NEX-Lama5*$^{-/-}$ mice here. Germline *Lama5* (Miner et al., 1998), *Itga3* (Kreidberg et al., 1996), and constitutive *Lamb2* mice (Noakes et al., 1995) were used for gene dosage experiments, and Thy1-GFPm mice (Feng et al., 2000) were used for dendritic spine visualization. All

procedures were compliant with federal regulations and approved by the Yale University Animal Care and Use Committee.

Laminin α5 Antibody

We raised an antibody to mouse laminin α5 in rabbit (Pocono Rabbit Farm) using a 285-amino-acid fragment from the L4a domain (amino acids 865–956) and affinity purified it according to standard protocols (Harlow and Lane, 1988). Membranes were probed with 0.4 μg/mL of this L4a laminin α5 antibody for 2–3 hr at 22°C in 5% BSA. We stained for laminin α5 in dissociated neurons and hippocampal tissue using 1–2 μg/mL of this antibody.

In Situ Hybridization

Laminin α5 mRNA was detected with a 755-bp complementary RNA probe (antisense) for bases 9,937–10,691 after the cDNA start codon, corresponding to the C-terminal globular domains, with the reverse sequence as a control probe (sense).

Dendritic Spine Motility Assay

DIV19–DIV23 dissociated hippocampal neurons plated on poly-D-lysine-coated glass-bottom culture dishes (MatTek) were imaged at 4-min intervals on a spinning disc confocal microscope. z stack series of a dendrite arbor were taken at 0.2 μm spacing for each time point from below detectable signal to above detectable signal to ensure dendritic spines were fully captured. For analysis, an investigator blinded to genotype and condition selected non-saturated spines with a spine neck visible between the spine head and the dendrite shaft. (Details on background subtraction, normalization, and quantification are in Supplemental Experimental Procedures.)

Electron Microscopy

Littermate mice were transcardially perfused with 4% paraformaldehyde and 2% glutaraldehyde. Synapses were identified as PSDs next to a plasma membrane apposed to vesicle-containing presynaptic compartment contained by a plasma membrane. Synapse densities were quantified per mouse using 500–1,000 μm^2 of CA1 stratum radiatum. PSD length was measured as the cross-sectional length of PSD in identified synapses. Spine head area was measured by tracing the plasma membrane of spines containing identified synapses that possessed a clear spine neck; area tracing included the entire spine down to the narrowest part of the spine neck.

mEPSCs

Whole-cell recordings were obtained from pyramidal neurons in hippocampal CA1 at room temperature. For AMPAR-mediated mEPSC recordings, 1 μM tetrodotoxin (TTX) was added to the external solution. To record NMDAR-mediated mEPSCs, neurons were held in voltage clamp at −40 mV in the presence of 1 μM TTX, 10 μM bicuculline methiodide (BMI), and 20 μM 6-cyano-7-nitroquinoxaline-2,3-dione (CNQX) in artificial cerebrospinal fluid (ACSF) with low Mg^{2+} (0.1 mm) and high Ca^{2+} (3.8 mm) to partially remove the Mg^{2+} block.

Statistical Analysis

Analysis was performed in Prism 7 software. When more than 2 groups were tested in the same experiment, ANOVA (or 2-way ANOVA) was used prior to any direct comparisons. For post hoc tests and groups of 2, methods of analysis were determined based on normality (using D'Agostino and Pearson and Shapiro-Wilk normality tests, which agreed in all uses here) and similarity of SD (using F tests) between groups. Mann-Whitney tests were used when skew was detected. Welch's correction was used for groups showing different SDs. For comparisons of dendritic spine fluctuation before and after treatments, we used Wilcoxon paired t tests. Specific details of n and statistical tests used are included in the figure legends.

Supplementary Material

Refer to Web version on PubMed Central for supplementary material.

Acknowledgments

The authors thank C. Kaliszewski, A.D. Levy, B. Rudeen, and X. Ye for assisting with experiments and A.D. Levy and S.M. Katrancha for helpful discussion and comments on the manuscript. Klaus-Armin Nave (Max Planck Institute of Experimental Medicine) generously provided the NEX-Cre mouse line. This work was supported by the NIH National Institute for Neurological Disorders and Stroke (grant NS089662 to A.J.K.; training grants GM007499 and NS007224 and predoctoral NRSA NS090767 to M.H.O.) and the NIH National Institute of Deafness and Other Communicative Disorders (grants DC013791 and DC012441 to C.A.G.).

References

Aumailley M. The laminin family. Cell Adhes. Migr. 2013; 7:48–55.

Beck K, Hunter I, Engel J. Structure and function of laminin: anatomy of a multidomain glycoprotein. FASEB J. 1990; 4:148–160. [PubMed: 2404817]

Bosch M, Hayashi Y. Structural plasticity of dendritic spines. Curr. Opin. Neurobiol. 2012; 22:383–388. [PubMed: 21963169]

Broadbent NJ, Gaskin S, Squire LR, Clark RE. Object recognition memory and the rodent hippocampus. Learn. Mem. 2009; 17:5–11. [PubMed: 20028732]

Campbell ID, Humphries MJ. Integrin structure, activation, and interactions. Cold Spring Harb. Perspect. Biol. 2011; 3:a004994. [PubMed: 21421922]

Chan CS, Weeber EJ, Zong L, Fuchs E, Sweatt JD, Davis RL. Beta 1-integrins are required for hippocampal AMPA receptor-dependent synaptic transmission, synaptic plasticity, and working memory. J. Neurosci. 2006; 26:223–232. [PubMed: 16399691]

Chan CS, Levenson JM, Mukhopadhyay PS, Zong L, Bradley A, Sweatt JD, Davis RL. Alpha3-integrins are required for hippocampal long-term potentiation and working memory. Learn. Mem. 2007; 14:606–615. [PubMed: 17848500]

Chen Z-L, Yu H, Yu W-M, Pawlak R, Strickland S. Proteo-lytic fragments of laminin promote excitotoxic neurodegeneration by up-regulation of the KA1 subunit of the kainate receptor. J. Cell Biol. 2008; 183:1299–1313. [PubMed: 19114596]

Chen CC, Lu J, Zuo Y. Spatiotemporal dynamics of dendritic spines in the living brain. Front. Neuroanat. 2014; 8:28. [PubMed: 24847214]

Cingolani LA, Thalhammer A, Yu LM, Catalano M, Ramos T, Colicos MA, Goda Y. Activity-dependent regulation of synaptic AMPA receptor composition and abundance by beta3 integrins. Neuron. 2008; 58:749–762. [PubMed: 18549786]

Cohen SJ, Munchow AH, Rios LM, Zhang G, Asgeirsdoóttir HN, Stackman RW Jr. The rodent hippocampus is essential for nonspatial object memory. Curr. Biol. 2013; 23:1685–1690. [PubMed: 23954431]

Colgan LA, Yasuda R. Plasticity of dendritic spines: subcompartmentalization of signaling. Annu. Rev. Physiol. 2014; 76:365–385. [PubMed: 24215443]

Colognato H, Yurchenco PD. Form and function: the laminin family of heterotrimers. Dev. Dyn. 2000; 218:213–234. [PubMed: 10842354]

Dailey ME, Smith SJ. The dynamics of dendritic structure in developing hippocampal slices. J. Neurosci. 1996; 16:2983–2994. [PubMed: 8622128]

Dziembowska M, Wlodarczyk J. MMP9: a novel function in synaptic plasticity. Int. J. Biochem. Cell Biol. 2012; 44:709–713. [PubMed: 22326910]

Engel J, Odermatt E, Engel A, Madri JA, Furthmayr H, Rohde H, Timpl R. Shapes, domain organizations and flexibility of laminin and fibronectin, two multifunctional proteins of the extracellular matrix. J. Mol. Biol. 1981; 150:97–120. [PubMed: 6795355]

Feng G, Mellor RH, Bernstein M, Keller-Peck C, Nguyen QT, Wallace M, Nerbonne JM, Lichtman JW, Sanes JR. Imaging neuronal subsets in transgenic mice expressing multiple spectral variants of GFP. Neuron. 2000; 28:41–51. [PubMed: 11086982]

Goebbels S, Bormuth I, Bode U, Hermanson O, Schwab MH, Nave KA. Genetic targeting of principal neurons in neocortex and hippocampus of NEX-Cre mice. Genesis. 2006; 44:611–621. [PubMed: 17146780]

Grutzendler J, Kasthuri N, Gan WB. Long-term dendritic spine stability in the adult cortex. Nature. 2002; 420:812–816. [PubMed: 12490949]

Harlow, E., Lane, D. Antibodies: A Laboratory Manual (Cold Spring Harbor Laboratory). 1988.

Hayashi-Takagi A, Yagishita S, Nakamura M, Shirai F, Wu YI, Losh-baugh AL, Kuhlman B, Hahn KM, Kasai H. Labelling and optical erasure of synaptic memory traces in the motor cortex. Nature. 2015; 525:333–338. [PubMed: 26352471]

Hernández SE, Settleman J, Koleske AJ. Adhesion-dependent regulation of p190RhoGAP in the developing brain by the Abl-related gene tyrosine kinase. Curr. Biol. 2004; 14:691–696. [PubMed: 15084284]

Holtmaat AJ, Trachtenberg JT, Wilbrecht L, Shepherd GM, Zhang X, Knott GW, Svoboda K. Transient and persistent dendritic spines in the neocortex in vivo. Neuron. 2005; 45:279–291. [PubMed: 15664179]

Huang Z, Shimazu K, Woo NH, Zang K, Müller U, Lu B, Reichardt LF. Distinct roles of the beta 1-class integrins at the developing and the mature hippocampal excitatory synapse. J. Neurosci. 2006; 26:11208–11219. [PubMed: 17065460]

Huntley GW. Synaptic circuit remodelling by matrix metalloproteinases in health and disease. Nat. Rev. Neurosci. 2012; 13:743–757. [PubMed: 23047773]

Hynes RO. Integrins: bidirectional, allosteric signaling machines. Cell. 2002; 110:673–687. [PubMed: 12297042]

Kapitein LC, Hoogenraad CC. Which way to go? Cytoskeletal organization and polarized transport in neurons. Mol. Cell. Neurosci. 2011; 46:9–20. [PubMed: 20817096]

Kapitein LC, Schlager MA, Kuijpers M, Wulf PS, van Spronsen M, MacKintosh FC, Hoogenraad CC. Mixed microtubules steer dynein-driven cargo transport into dendrites. Curr. Biol. 2010; 20:290–299. [PubMed: 20137950]

Kerrisk ME, Greer CA, Koleske AJ. Integrin α3 is required for late postnatal stability of dendrite arbors, dendritic spines and synapses, and mouse behavior. J. Neurosci. 2013; 33:6742–6752. [PubMed: 23595732]

Kreidberg JA, Donovan MJ, Goldstein SL, Rennke H, Shepherd K, Jones RC, Jaenisch R. Alpha 3 beta 1 integrin has a crucial role in kidney and lung organogenesis. Development. 1996; 122:3537–3547. [PubMed: 8951069]

Lai KO, Ip NY. Structural plasticity of dendritic spines: the underlying mechanisms and its dysregulation in brain disorders. Biochim. Bio-phys. Acta. 2013; 1832:2257–2263.

Lévi S, Grady RM, Henry MD, Campbell KP, Sanes JR, Craig AM. Dystroglycan is selectively associated with inhibitory GABAergic synapses but is dispensable for their differentiation. J. Neurosci. 2002; 22:4274–4285. [PubMed: 12040032]

Levy AD, Omar MH, Koleske AJ. Extracellular matrix control of dendritic spine and synapse structure and plasticity in adulthood. Front. Neuroanat. 2014; 8:116. [PubMed: 25368556]

Magnowska M, Gorkiewicz T, Suska A, Wawrzyniak M, Rutkowska-Wlodarczyk I, Kaczmarek L, Wlodarczyk J. Transient ECM protease activity promotes synaptic plasticity. Sci. Rep. 2016; 6:27757. [PubMed: 27282248]

Majewska A, Sur M. Motility of dendritic spines in visual cortex in vivo: changes during the critical period and effects of visual deprivation. Proc. Natl. Acad. Sci. USA. 2003; 100:16024–16029. [PubMed: 14663137]

Martin PT, Ettinger AJ, Sanes JR. A synaptic localization domain in the synaptic cleft protein laminin beta 2 (s-laminin). Science. 1995; 269:413–416. [PubMed: 7618109]

Matsuzaki M, Honkura N, Ellis-Davies GC, Kasai H. Structural basis of long-term potentiation in single dendritic spines. Nature. 2004; 429:761–766. [PubMed: 15190253]

Michaluk P, Mikasova L, Groc L, Frischknecht R, Choquet D, Kaczmarek L. Matrix metalloproteinase-9 controls NMDA receptor surface diffusion through integrin beta1 signaling. J. Neurosci. 2009; 29:6007–6012. [PubMed: 19420267]

Miner JH, Cunningham J, Sanes JR. Roles for laminin in embryogenesis: exencephaly, syndactyly, and placentopathy in mice lacking the laminin α5 chain. J. Cell Biol. 1998; 143:1713–1723. [PubMed: 9852162]

Mortillo S, Elste A, Ge Y, Patil SB, Hsiao K, Huntley GW, Davis RL, Benson DL. Compensatory redistribution of neuroligins and N-cadherin following deletion of synaptic β1-integrin. J. Comp. Neurol. 2012; 520:2041–2052. [PubMed: 22488504]

Moulson CL, Li C, Miner JH. Localization of Lutheran, a novel laminin receptor, in normal, knockout, and transgenic mice suggests an interaction with laminin α5 in vivo. Dev. Dyn. 2001; 222:101–114. [PubMed: 11507772]

Murthy VN, Schikorski T, Stevens CF, Zhu Y. Inactivity produces increases in neurotransmitter release and synapse size. Neuron. 2001; 32:673–682. [PubMed: 11719207]

Nägerl UV, Eberhorn N, Cambridge SB, Bonhoeffer T. Bidirectional activity-dependent morphological plasticity in hippocampal neurons. Neuron. 2004; 44:759–767. [PubMed: 15572108]

Nguyen NM, Kelley DG, Schlueter JA, Meyer MJ, Senior RM, Miner JH. Epithelial laminin alpha5 is necessary for distal epithelial cell maturation, VEGF production, and alveolization in the developing murine lung. Dev. Biol. 2005; 282:111–125. [PubMed: 15936333]

Nishimune H, Sanes JR, Carlson SS. A synaptic laminin-calcium channel interaction organizes active zones in motor nerve terminals. Nature. 2004; 432:580–587. [PubMed: 15577901]

Nishimune H, Valdez G, Jarad G, Moulson CL, Müller U, Miner JH, Sanes JR. Laminins promote postsynaptic maturation by an autocrine mechanism at the neuromuscular junction. J. Cell Biol. 2008; 182:1201–1215. [PubMed: 18794334]

Nishiuchi R, Takagi J, Hayashi M, Ido H, Yagi Y, Sanzen N, Tsuji T, Ya-mada M, Sekiguchi K. Ligand-binding specificities of laminin-binding integrins: a comprehensive survey of laminin-integrin interactions using recombinant alpha3beta1, alpha6beta1, alpha7beta1 and alpha6beta4 integrins. Matrix Biol. 2006; 25:189–197. [PubMed: 16413178]

Noakes PG, Gautam M, Mudd J, Sanes JR, Merlie JP. Aberrant differentiation of neuromuscular junctions in mice lacking s-laminin/ laminin beta 2. Nature. 1995; 374:258–262. [PubMed: 7885444]

Oray S, Majewska A, Sur M. Dendritic spine dynamics are regulated by monocular deprivation and extracellular matrix degradation. Neuron. 2004; 44:1021–1030. [PubMed: 15603744]

Park YK, Goda Y. Integrins in synapse regulation. Nat. Rev. Neu-rosci. 2016; 17:745–756.

Patton BL, Miner JH, Chiu AY, Sanes JR. Distribution and function of laminins in the neuromuscular system of developing, adult, and mutant mice. J. Cell Biol. 1997; 139:1507–1521. [PubMed: 9396756]

Patton BL, Chiu AY, Sanes JR. Synaptic laminin prevents glial entry into the synaptic cleft. Nature. 1998; 393:698–701. [PubMed: 9641682]

Patton BL, Cunningham JM, Thyboll J, Kortesmaa J, Westerblad H, Edström L, Tryggvason K, Sanes JR. Properly formed but improperly localized synaptic specializations in the absence of laminin alpha4. Nat. Neurosci. 2001; 4:597–604. [PubMed: 11369940]

Pozo K, Cingolani LA, Bassani S, Laurent F, Passafaro M, Goda Y. β3 integrin interacts directly with GluA2 AMPA receptor subunit and regulates AMPA receptor expression in hippocampal neurons. Proc. Natl. Acad. Sci. USA. 2012; 109:1323–1328. [PubMed: 22232691]

Roberts TF, Tschida KA, Klein ME, Mooney R. Rapid spine stabilization and synaptic enhancement at the onset of behavioural learning. Nature. 2010; 463:948–952. [PubMed: 20164928]

Rogers RS, Nishimune H. The role of laminins in the organization and function of neuromuscular junctions. Matrix Biol. 2017; 57–58:86–105.

Sanes JR. The basement membrane/basal lamina of skeletal muscle. J. Biol. Chem. 2003; 278:12601–12604. [PubMed: 12556454]

Sfakianos MK, Eisman A, Gourley SL, Bradley WD, Scheetz AJ, Settleman J, Taylor JR, Greer CA, Williamson A, Koleske AJ. Inhibition of Rho via Arg and p190RhoGAP in the postnatal mouse hippocampus regulates dendritic spine maturation, synapse and dendrite stability, and behavior. J. Neurosci. 2007; 27:10982–10992. [PubMed: 17928439]

Shi Y, Ethell IM. Integrins control dendritic spine plasticity in hippocampal neurons through NMDA receptor and Ca2+/calmodulin-dependent protein kinase II-mediated actin reorganization. J. Neurosci. 2006; 26:1813–1822. [PubMed: 16467530]

Simpson MA, Bradley WD, Harburger D, Parsons M, Calderwood DA, Koleske AJ. Direct interactions with the integrin β1 cytoplasmic tail activate the Abl2/Arg kinase. J. Biol. Chem. 2015; 290:8360–8372. [PubMed: 25694433]

Tropea D, Majewska AK, Garcia R, Sur M. Structural dynamics of synapses in vivo correlate with functional changes during experience-dependent plasticity in visual cortex. J. Neurosci. 2010; 30:11086–11095. [PubMed: 20720116]

Tsai P-I, Wang M, Kao H-H, Cheng Y-J, Lin Y-J, Chen R-H, Chien C-T. Activity-dependent retrograde laminin A signaling regulates synapse growth at Drosophila neuromuscular junctions. Proc. Natl. Acad. Sci. USA. 2012; 109:17699–17704. [PubMed: 23054837]

Vezina-Audette R, Tremblay M, Carbonetto S. Laminin is instructive and calmodulin dependent kinase II is non-permissive for the formation of complex aggregates of acetylcholine receptors on myotubes in culture. Matrix Biol. 2017; 57–58:106–123.

Warren MS, Bradley WD, Gourley SL, Lin YC, Simpson MA, Reichardt LF, Greer CA, Taylor JR, Koleske AJ. Integrin β1 signals through Arg to regulate postnatal dendritic arborization, synapse density, and behavior. J. Neurosci. 2012; 32:2824–2834. [PubMed: 22357865]

Wlodarczyk J, Mukhina I, Kaczmarek L, Dityatev A. Extracellular matrix molecules, their receptors, and secreted proteases in synaptic plasticity. Dev. Neurobiol. 2011; 71:1040–1053. [PubMed: 21793226]

Yao Y. Laminin: loss-of-function studies. Cell. Mol. Life Sci. 2017; 74:1095–1115. [PubMed: 27696112]

Yoshihara Y, De Roo M, Muller D. Dendritic spine formation and stabilization. Curr. Opin. Neurobiol. 2009; 19:146–153. [PubMed: 19523814]

Yurchenco PD. Basementmembranes: cell scaffoldings and signaling platforms. Cold Spring Harb. Perspect. Biol. 2011; 3:a004911. [PubMed: 21421915]

Yurchenco PD, Schittny JC. Molecular architecture of basement membranes. FASEB J. 1990; 4:1577–1590. [PubMed: 2180767]

Zhou Q, Homma KJ, Poo MM. Shrinkage of dendritic spines associated with long-term depression of hippocampal synapses. Neuron. 2004; 44:749–757. [PubMed: 15572107]

Zuo Y, Lin A, Chang P, Gan WB. Development of long-term dendritic spine stability in diverse regions of cerebral cortex. Neuron. 2005; 46:181–189. [PubMed: 15848798]

Highlights

- Neurons express the ECM protein laminin α5 and deposit it at synapses in the brain
- An α5-laminin is necessary and sufficient to stabilize dendritic spine dynamics
- Laminin α5 loss disrupts synapse density, synaptic transmission, and behavior
- Laminin α5 signals through integrin α3β1-Abl2-p190RhoGAP in the brain

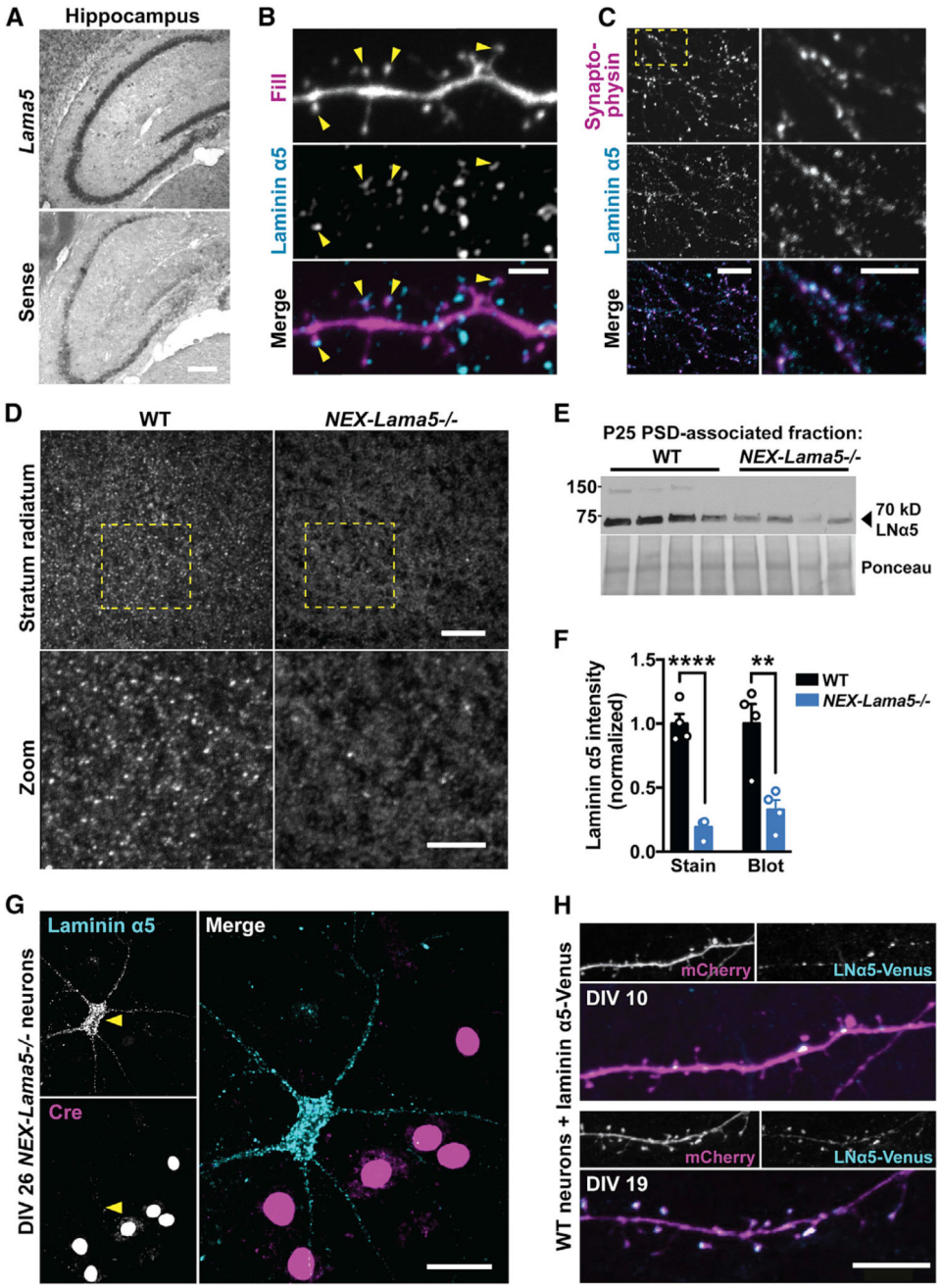

Figure 1. Laminin α5 Is Deposited at Synapses by Hippocampal Neurons

(A) In situ hybridization with *Lama5* antisense probe (top) or reverse complement (bottom) in hippocampus from P35 wild-type (WT) mice reveals strong *Lama5* signal in the pyramidal layer and scattered cells in the strata oriens and lacunosum moleculare. Scale bar, 100 μm. See Figure S1A for cortex and cerebellum.

(B) Live (extracellular) immunostaining for laminin α5 along a GFP-labeled dendrite from 21 days *in vitro* (DIV21) dissociated WT hippocampus. Laminin α5 was detected at tips of dendritic spine heads (yellow arrowheads). Scale bar, 2 μm.

(C) Co-staining of DIV19 WT hippocampal neurons for synaptophysin (magenta) and laminin α5 (cyan) shows laminin α5 clusters at synaptophysin-positive sites. Dashed box on the top left is enlarged in the series to the right. Scale bars represent 10 μm (left) and 5 μm (right).

(D) Immunostaining for laminin α5 in CA1 stratum radiatum of P30 WT (left) and excitatory neuron-specific laminin α5 KO mice (NEX-Cre; *Lama5*$^{flox/flox}$*NEX-Lama5*$^{-/-}$) (right) shows reduced staining for laminin α5 in *NEX-Lama5*$^{-/-}$ sections. Boxed regions are enlarged in bottom panels. Fluorescence intensity is quantified in (F) (left). Scale bars represent 10 μm (top) and 5 μm (bottom).

(E) Immunoblot of the PSD fraction of hippocampus from 4 WT and 4 *NEX-Lama5*$^{-/-}$ P25 mice. Intensity of signals were normalized to total protein per lane, visualized by Ponceau S (Ponceau) stain. Faint bands in the *NEX-Lama5*$^{-/-}$ mice likely result from the non-recombined laminin α5 in inhibitory cells (G). Signal intensity is quantified in (F) (right). See Figure S1 for blots of all fractions and time course.

(F) Hippocampal laminin α5 staining (left) and PSD-associated 70-kDa laminin α5 (right) are decreased by 79% and 70% in *NEX-Lama5*$^{-/-}$mice, respectively. Residual signals are likely laminin α5 from inhibitory neurons. n = 4 images (stain) and 4 mice (blot). Data are presented as mean + SEM. **$p < 0.01$; ****$p < 0.0001$ (unpaired t test).

(G) DIV26 neurons cultured from *NEX-Lama5*$^{-/-}$ mice were stained for laminin α5 and Cre. A Cre-negative cell (yellow arrowhead) has a strong punctate laminin α5 signal, while Cre-positive cells show no signal. Scale bar, 20 μm (bottom) and 40 μm (top). (H) Expression of cytosolic mCherry and a G2-domain-tagged laminin α5 construct in dissociated hippocampal neurons at two ages. At DIV 10, laminin is localized to the base of spines; at DIV 19, the protein is detected at the tips of spine heads. Scale bar, 10 μm. See Figure S2 for related experiments.

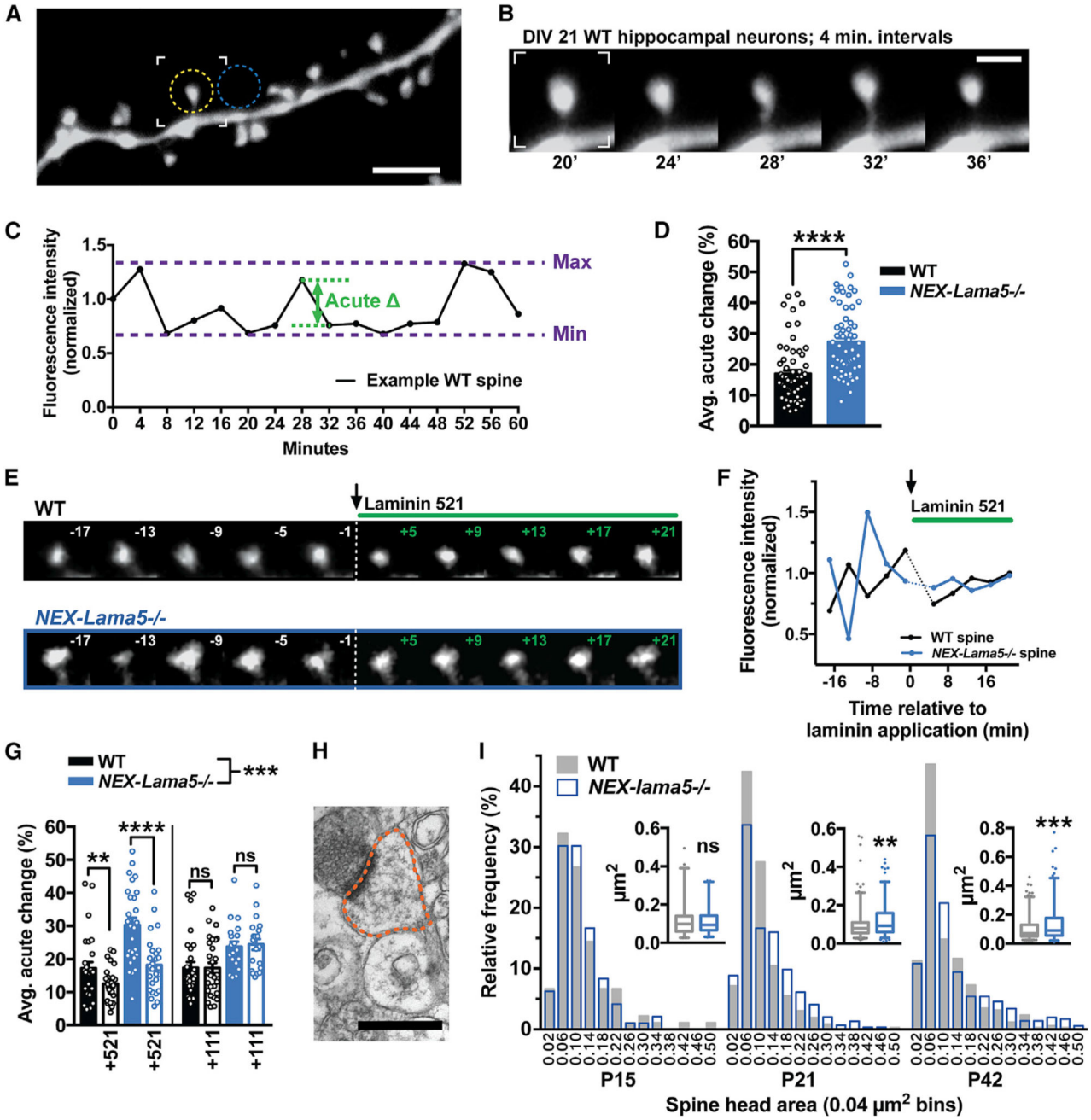

Figure 2. Laminin α5 Attenuates Dendritic Spine Structural Dynamics and Regulates Spine Head Size

(A) Example dendrite segment from a WT hippocampal neuron at DIV21. Dashed circles indicate ROIs used to quantify fluorescence intensity (yellow) and background (blue). The white square is featured in (B). Scale bar, 5 μm.

(B) Magnification of spine from (A). Fluorescence intensity was measured every 4 min; time below is relative to the start of the imaging session. Scale bar, 2 μm.

(C) Black line depicts example fluctuation of fluorescence intensity over time, normalized to the average intensity for that spine and the intensity for the entire dendrite arbor (see Experimental Procedures). The purple dashed lines represent the range values used to

determine maximum fold change (quantified in Figure S3). The green dashed lines represent measurements used to determine acute percent change for each time point ($|[Intensity_t - Intensity_{t-1}]/Intensity_{t-1}| \times 100$). 4-min changes are averaged over the imaging session for each spine to yield one data point in (D) and (G).

(D) Fluorescence intensity of spines from *NEX-Lama5*$^{-/-}$ neurons changes more within each 4-min interval versus WT; n = 67 (WT) and 62 (*NEX-Lama5*$^{-/-}$) spines from 4 cultures each. See Figure S3 for fold-change data. Data are presented as mean ± SEM. WT condition displayed skewed distribution, so the Mann-Whitney test was used to determine statistical significance (****$p < 0.0001$).

(E) Representative spines from a WT (top) and *NEX-Lama5*$^{-/-}$ (bottom) neuron before and after 3 nM laminin 521 application. White and green numbers are minutes relative to laminin addition. The dotted line separates pre- and post-laminin 521.

(F) Quantification of fluorescence for the example spines in (E). Dotted lines represent a 5-min break in imaging after laminin is added. Intensity values were normalized to average spine intensity for each imaging session.

(G) Application of laminin 521, but not 111, decreases 4-min fluctuations of fluorescence intensity in *NEX-Lama5*$^{-/-}$ spines; n = 21–28 spines, 2 cultures per condition. Data are presented as mean ± SEM; 2-way ANOVA identified an effect of genotype for all conditions, confirming results in (D), and identified an effect of 521, but not 111. Wilcoxon paired test revealed significant differences between before and after 521 for both WT and *NEX-Lama5*$^{-/-}$ conditions and no significant differences for 111 (**$p < 0.01$; ***$p < 0.001$; ****$p < 0.0001$). See Figure S3 for laminin effects on overall fold change and experiments with laminin 332.

(H) Orange outline represents area quantified from an EM image for a representative dendritic spine head. Scale bar, 500 nm.

(I) Spine head area is not different at P15, but increased in *NEX-Lama5*$^{-/-}$ mice versus WT littermates at P21 and P42 (insets) (**$p < 0.01$; ***$p < 0.001$; Mann-Whitney test), with an observable broadening of the distribution for *NEX-Lama5*$^{-/-}$ versus WT (F test analysis of variance; $p < 0.01$ for P21 and $p < 0.0001$ for P42). Insets show median, quartiles and 2.5%–97.5% range with 2.5% tails as dots. Individual spine head measurements were binned at 0.04 μm^2; n = 294–363 spines from 3 mice for P21 and P42, n = 90 spines from 2 mice for P15.

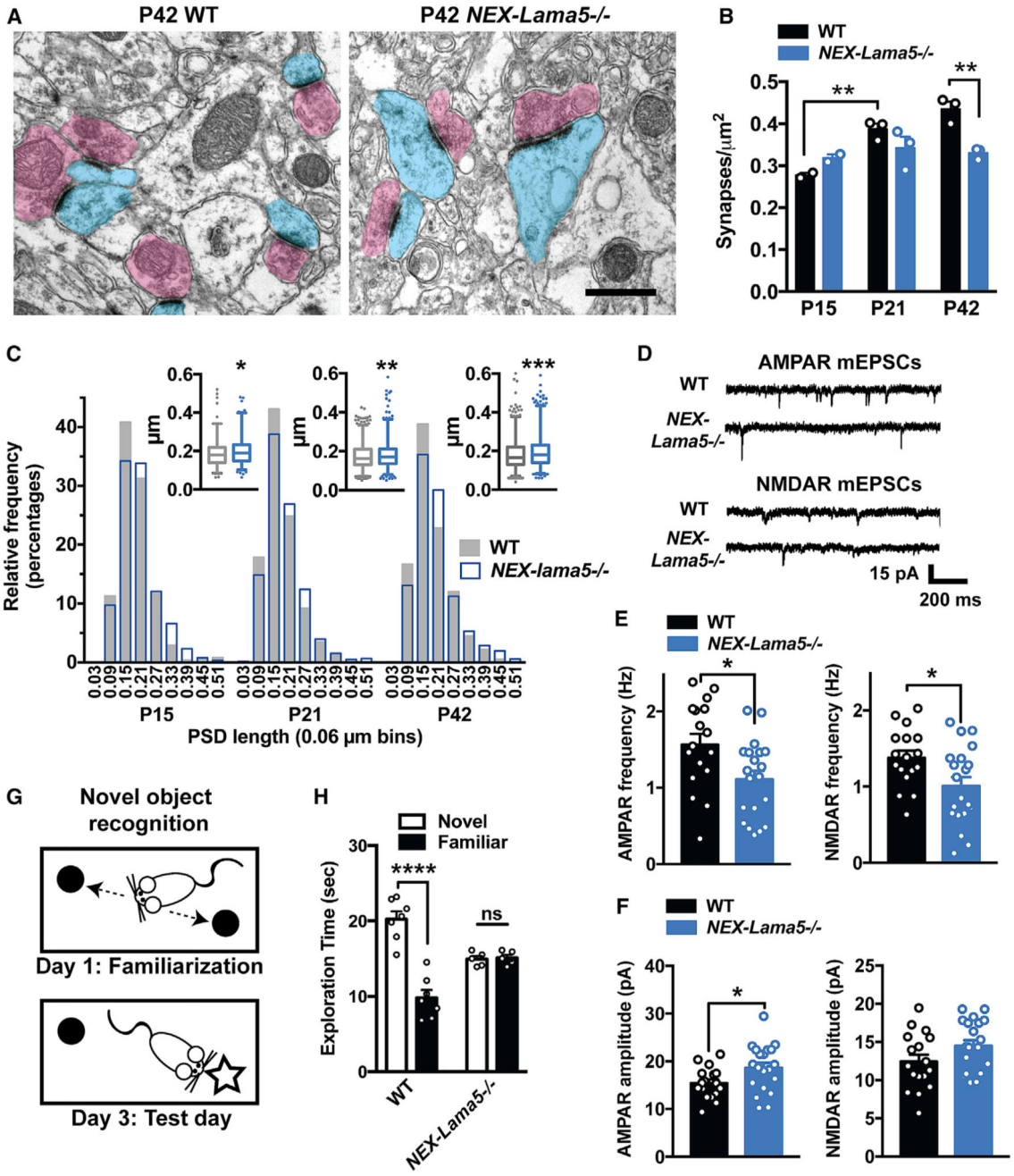

Figure 3. Loss of Laminin α5 from Excitatory Neurons Disrupts Hippocampal Synapses and Animal Behavior

(A) Representative micrographs from hippocampal CA1 stratum radiatum of P42 WT (left) and *NEX-Lama5*$^{-/-}$ (right) littermates. Excitatory synapses are pseudocolored blue (postsynaptic) and pink (presynaptic). Scale bar, 500 nm.

(B) Quantification of synapses per square micrometer reveals a 24% decrease in synapses in *NEX-Lama5*$^{-/-}$ mice at P42 but no difference at P15 or P21. Additionally, from P15 to P21, density increases 40% in WT but does not change in *NEX-Lama5*$^{-/-}$ mice; n = 3 male littermate pairs for P21 and P42, n = 2 male littermate pairs for P15. Data are presented as

mean + SEM; 2-way ANOVA with a post hoc Sidak's multiple comparisons test (**p < 0.01).

(C) Length of PSDs is significantly increased in *NEX-Lama5*$^{-/-}$ mice at all ages relative to WT littermates (shown as a right shift in the distributions). Difference in means: P15 = +8%, P21 = +5%; P42 = +9%; n = 580–829 synapses from 3 mice for P21 and P42, n = 240–257 synapses from 2 mice for P15. Inset shows median, quartiles, and 2.5%–97.5% range with 2.5% tails as dots. *p < 0.05; **p < 0.01; ***p < 0.001 (Mann-Whitney test).

(D) Representative AMPAR and NMDAR miniature excitatory postsynaptic current recordings (mEPSCs) from CA1 of P31 WT and NEX-*Lama5*$^{-/-}$ mice.

(E and F) Frequency (E) of AMPA (left) and NMDAR (right) mEPSCs are reduced in *NEX-Lama5*$^{-/-}$ mice relative to WT controls, consistent with synapse reduction observed ultrastructurally in (B). Amplitudes (F) of AMPAR mEPSCs (left) were increased in *NEX-Lama5*$^{-/-}$ mice relative to WT, but NMDAR (right) mEPSC amplitudes were unaffected. n = 17 WT and 20 *NEX-Lama5*$^{-/-}$ neurons from 5 male mice each. Data are presented as mean + SEM. *p < 0.05 (unpaired t test).

(G) The novel object recognition task quantifies preference for a new object versus a familiar object. See Supplemental Experimental Procedures for description and Figure S4 for control measurements.

(H) Percentage of tactile exploration time of the familiar and novel objects. P42 WT mice show a clear preference for the novel object, while their *NEX-Lama5*$^{-/-}$littermates do not; n = 7 WT and n = 5 *NEX-Lama5*$^{-/-}$ littermate males. Data are presented as mean ± SEM. Multiple t tests using the Holm-Sidak method were used to compare time spent with novel versus familiar objects in both genotype groups (****p < 0.0001).

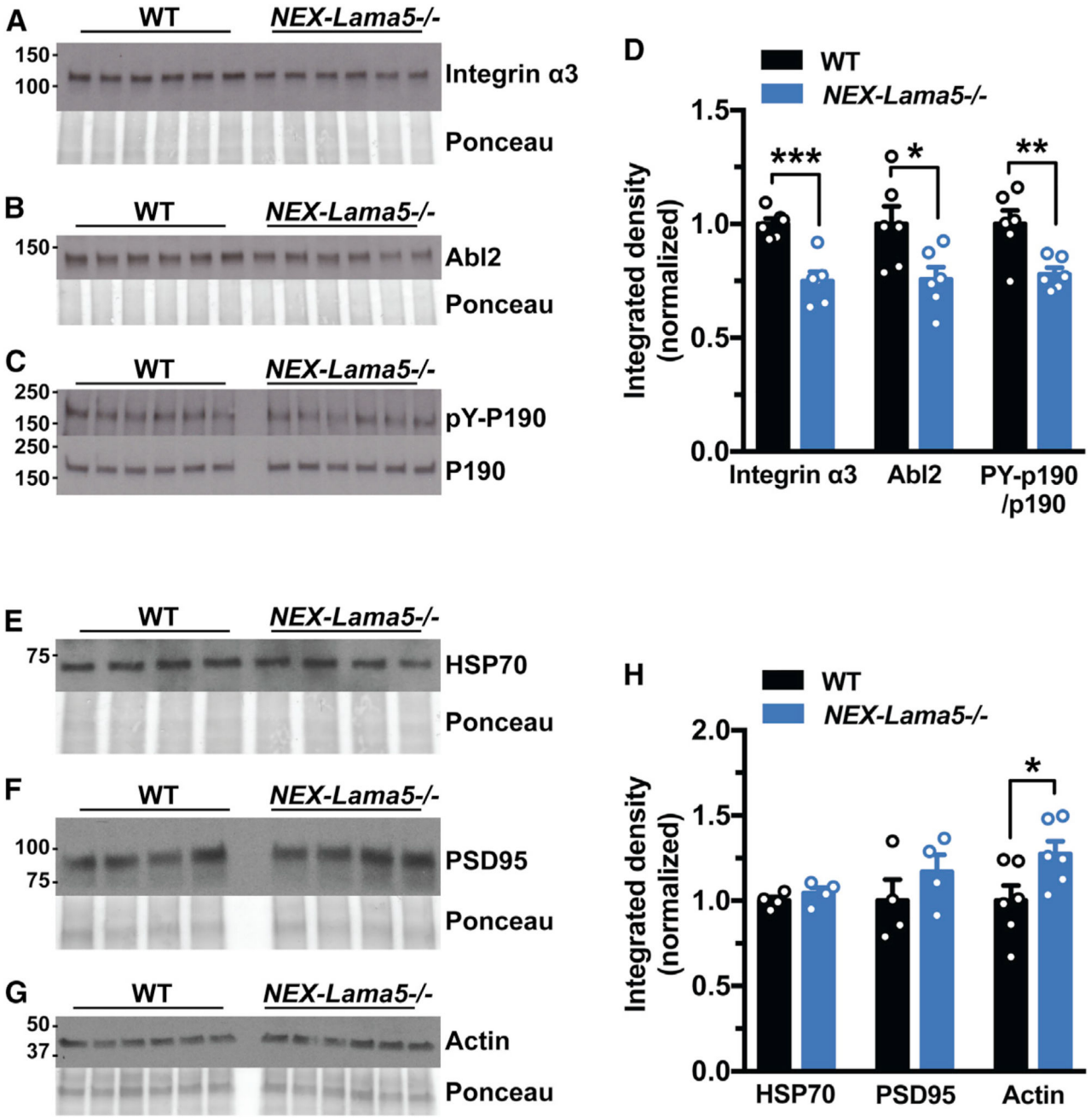

Figure 4. Loss of Laminin α5 Disrupts Integrin-Abl2-p190RhoGAP Signaling

(A and B) Images show immunoblots probing for integrin α3 (A) and Abl2/Arg (Abl2) levels in hippocampal synaptosomes from P21 WT and *NEX-Lama5*$^{-/-}$ mice. Ponceau-S-stained membranes were used to normalize the signal to total protein loaded.

(C) Images of western blots for tyrosine phosphorylation (top) and total levels (bottom) of the Arg kinase substrate p190RhoGAP in hippocampal PSD-associated fractions from P21 *NEX-Lama5*$^{-/-}$ and WT mice. A demonstration that the phosphotyrosine antibody is detecting p190RhoGAP is shown in Figure S5.

(D) Integrin α3, Abl2, and relative p190RhoGAP phosphorylation (phosphotyrosine-p190RhoGAP/ total p190RhoGAP) are decreased by 25%, 24%, and 22%, respectively, in *NEX-Lama5*$^{-/-}$ mice compared to WT; n = 6. Data are presented as mean ± SEM. Data were analyzed using unpaired t tests (*p < 0.05; **p < 0.01; ***p < 0.001).

(E–G) Images of western blots show levels of HSP70 (E) in synaptosomal fractions and PSD95 (F) and actin (G) in PSD fractions from hippocampus of P21 mice.

(H) HSP70 and PSD95 levels are unchanged and actin levels are increased by 27% in *NEX-Lama5*$^{-/-}$ mice compared to WT mice. Graph shows quantitation relative to total protein (Ponceau stain). These measurements demonstrate that the decreases found in (A)–(D) are selective. The increase in actin levels is consistent with larger spine heads and PSDs in *NEX-Lama5*$^{-/-}$ mice at P21 (Figures 2I and 3C); n = 4–6 mice. Data are presented as mean ± SEM. Statistical significance was determined using unpaired t tests (*p < 0.05).

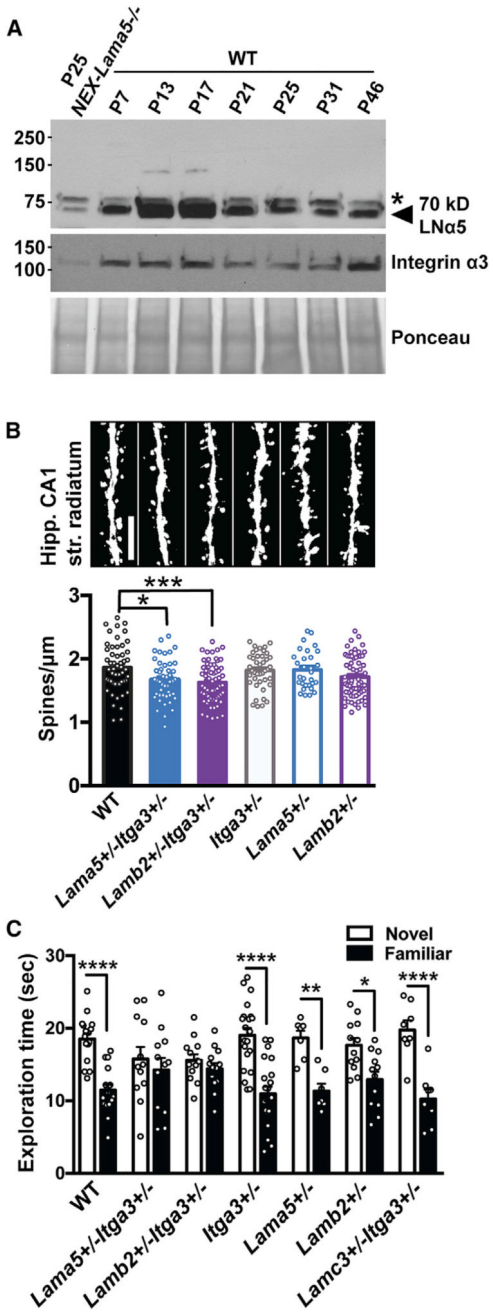

Figure 5. Laminin α5 Interacts Functionally with Integrin α3 to Regulate Spine Density and Animal Behavior

(A) Laminin α5 and integrin α3 co-express in a developmental time course. Image shows western blots of laminin α5 (top) and integrin α3 (mid) levels in hippocampal synaptosomes through mid and late postnatal development. The two proteins show similar peaks in expression at P17 followed by a reduction. A similar time course is shown in (Figure S1D). The asterisk indicates the non-neuronal or non-specific band described in Figure S1.

(B) Images show representative CA1 secondary apical dendrite segments from P42 male mice used in genetic interaction experiments (top). Scale bar, 5 µm. *Lama5*$^{+/-}$ *Itga3*$^{+/-}$ and *Lamb2*$^{+/-}$ *Itga3*$^{+/-}$ double heterozygotes have lower spine density than WT mice, while

single heterozygotes do not exhibit significant differences (bottom); n = 30–65 dendrite segments from 4–8 mice. Data are presented as mean ± SEM. One-way ANOVA identified differences within the group, and Sidak's multiple comparisons test was used for post hoc analysis (*p < 0.05; ***p < 0.001).

(C) *Lama5*$^{+/-}$*Itga3*$^{+/-}$ and *Lamb2*$^{+/-}$*Itga3*$^{+/-}$ double heterozygotes fail to prefer the novel object, while WT mice, single heterozygotes, and *Lamc3*$^{+/-}$*Itga3*$^{+/-}$ mice all prefer the novel object. Data are presented as mean ± SEM. Multiple t tests using the Holm-Sidak method were used to compare time spent with novel versus familiar objects in all genotype groups (*p < 0.05; **p < 0.01; ****p < 0.0001).

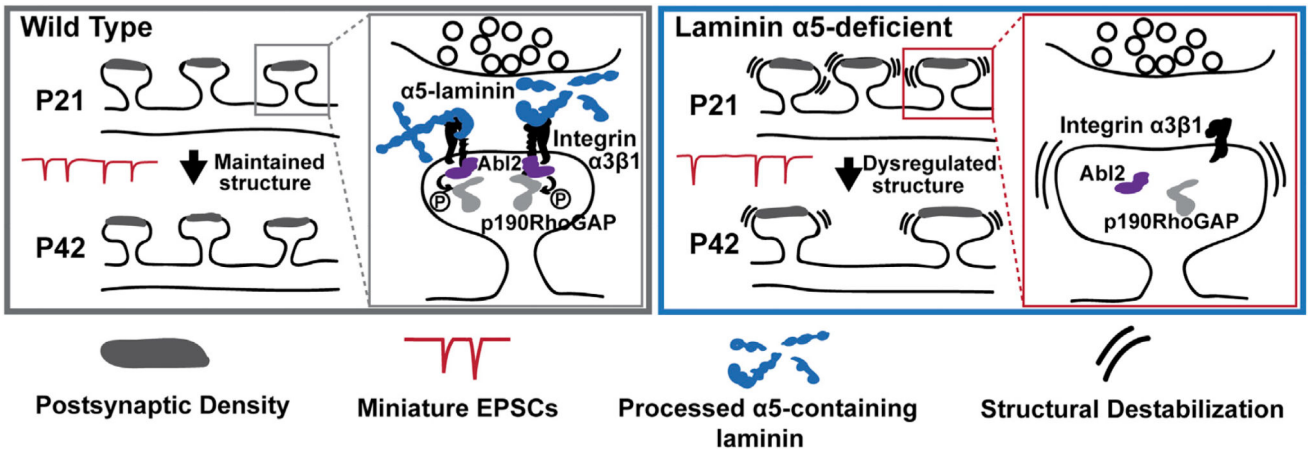

Figure 6. Summary Model: Laminin α5 Control of Hippocampal Synapse Stability

In WT mice, dendritic spines and PSDs maintain their size and density between P21 and P42 via a laminin-integrin signaling interaction (left). In this model, an α5-containing laminin engages integrin α3β1 to activate downstream signaling between Abl2/Arg kinase and p190RhoGAP. The α5-containing laminin trimer may be proteolytically processed to allow its integration into the synapse. Loss of laminin α5 from the postsynaptic cell causes both structural and functional defects at hippocampal synapses between P21 and P42 (right). Integrin α3β1 receptors and Abl2 are less active, which results in less phosphorylated p190RhoGAP. Synapse structure is dysregulated, yielding more motile spines with larger spine heads and PSDs at both time points and fewer synapses by P42.